Discovery, Optimization, and Pharmacological Characterization of Novel Heteroaroylphenylureas Antagonists of C−C Chemokine Ligand 2 Function[†]

Edgardo Laborde,*,[‡] Robert W. Macsata,[‡] Fanying Meng,[‡] Brian T. Peterson,[‡] Louise Robinson,[‡] Steve R. Schow,[‡] Reyna J. Simon,[‡] Hua Xu,[‡] Kunihisa Baba,[§] Hideaki Inagaki,[§] Yoshiro Ishiwata,[§] Takahito Jomori,[§] Yukiharu Matsumoto,[§] Atsushi Miyachi,[§] Takashi Nakamura,[§] Masayuki Okamoto,[§] Tracy M. Handel,[‖] and Claude C. A. Bernard[⊥]

[‡]Telik, Inc., 700 Hansen Way, Palo Alto, California 94304, United States

[§]Sanwa Kagaku Kenkyusho Co., Ltd., Mie Research Park, 363 Shiosaki, Hokusei-Cho, Inabe-Shi, Mie, 511-0406, Japan

[‖]Skaggs School of Pharmacy and Pharmaceutical Sciences, University of California San Diego, 9500 Gilman Drive, La Jolla, California 92093, United States

[⊥]Immunology and Stem Cell Laboratories, Monash University, Building 75, Wellington Road, Clayton, Victoria 3800, Australia

S Supporting Information

ABSTRACT: Through the application of TRAP (target-related affinity profiling), we identified a novel class of heteroaroylphenylureas that inhibit human CCL2-induced chemotaxis of monocytes/macrophages both in vitro and in vivo. This inhibition was concentration-dependent and selective with regard to other chemokines. The compounds, however, did not antagonize the binding of ^{125}I-labeled CCL2 to the CCR2 receptor nor did they block CCR2-mediated signal transduction responses such as calcium mobilization. Optimization of early leads for potency and pharmacokinetic parameters resulted in the identification of **17**, a potent inhibitor of chemotaxis (IC_{50} = 80 nM) with excellent oral bioavailability in rats (F = 60%). Compound **17** reduced swelling and joint destruction in two rat models of rheumatoid arthritis and delayed disease onset and produced near complete resolution of symptoms in a mouse model of multiple sclerosis.
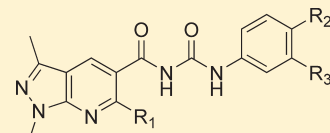
■ INTRODUCTION

The migration of leukocytes from blood vessels into diseased tissues is an important process in the initiation of normal inflammatory responses to certain stimuli or insults to the immune system. However, this process is also involved in the onset and progression of life-threatening inflammatory and autoimmune diseases, suggesting that blocking leukocyte recruitment in these disease states may be an effective therapeutic strategy.

The mechanism by which leukocytes leave the bloodstream and accumulate at sites of inflammation encompasses at least three distinct steps: (1) rolling along the vasculature, (2) arrest and firm adhesion, and (3) transendothelial migration.[1−5] The second and third steps are mediated by proinflammatory cytokines, adhesion molecules, and chemokines (chemoattractant cytokines), low-molecular-weight proteins secreted by proinflammatory cells at the site of damage or infection that stimulate directed cell migration or chemotaxis.[6−8] The biological actions of chemokines are mediated through their binding to specific G-protein-coupled receptors (GPCRs) on the leukocyte surface. This binding activates signaling pathways that lead to an increase in leukocyte adhesion to the endothelium and subsequent transmigration into the affected tissue.[9,10]

C−C chemokine ligand 2 (CCL2, previously referred to as monocyte chemoattractant protein 1 or MCP-1) was one of the first chemokines to be characterized biologically.[11,12] It is a member of the C−C chemokine subfamily and acts primarily through the C−C chemokine receptor 2 (CCR2) to recruit monocytes, basophils, and T-cells to sites of inflammation.[13] CCL2 has been implicated as an important mediator of several diseases, including multiple sclerosis,[14−16] rheumatoid arthritis,[17−19] and atherosclerosis.[20−22] Therefore, drugs that selectively block CCL2-induced leukocyte recruitment in these diseases may hold significant therapeutic potential.[23−25] This premise prompted the search in recent years for small-molecule CCR2 antagonists that would compete with CCL2 for binding to the receptor without inducing a functional response. These efforts identified several potent compounds, some of which showed significant therapeutic activity in animal models of inflammation. A number of these agents have advanced to clinical trials in humans, where they have met with various degrees of success.[26] We report herein the discovery and optimization of a series of heteroaroylphenylureas that inhibit CCL2-induced chemotaxis of monocytes/macrophages both in vitro and in vivo but do not antagonize the binding of CCL2 to the CCR2 receptor. In particular, compound **17** was identified as a potent and selective chemotaxis inhibitor with significant oral efficacy in animal models of rheumatoid arthritis and multiple sclerosis.
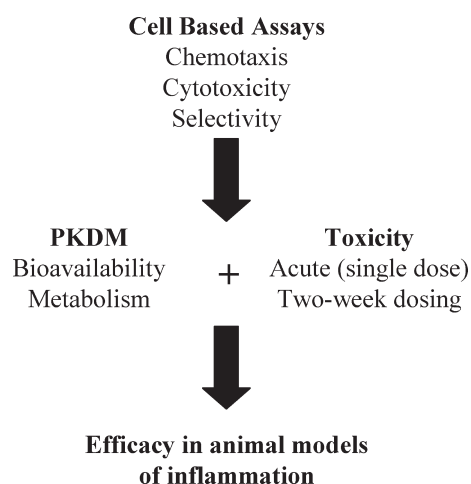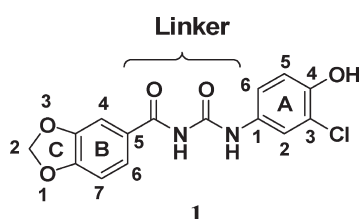
Figure 1. Lead optimization strategy.

Figure 2. Structure of compound **1**.

■ LEAD DISCOVERY AND OPTIMIZATION

Most of the research programs aimed at discovering small-molecule CCR2 antagonists have been initiated by screening compounds for their ability to disrupt binding of the human CCL2 ligand to the human CCR2 receptor. Although this strategy identified potent antagonists in vitro, several of these compounds later showed low selectivity over other GPCRs, poor correlation between binding affinity and functional activity, or lack of pharmacological action in animal models of inflammation. To circumvent these difficulties, we used a functional assay involving inhibition of CCL2-induced chemotaxis as our initial screening platform and tested compounds in vivo as expeditiously as possible to determine whether functional activity correlated with pharmacological activity. The lead optimization strategy implemented throughout our program is shown in (Figure 1).

Compounds active in the chemotaxis assay (IC$_{50}$ < 1 μM) were screened for cytotoxicity to distinguish between inhibition of cell migration and overt cell toxicity and for selectivity toward other chemokines. Those compounds with a good safety index (defined as the ratio of CC$_{50}$ to IC$_{50}$) and high selectivity were then tested in vivo to assess their pharmacokinetic−drug metabolism (PKDM) and toxicity profiles and finally in animal models of inflammation.

The initial lead, compound **1** (Figure 2), was discovered using TRAP (target-related affinity profiling), Telik's highly efficient drug discovery technology.[27] As TRAP identifies druglike leads with the screening of as few as 200 compounds, it is well suited to complex biological assays such as the inhibition of cell migration. Selected compounds were tested for their ability to inhibit hCCL2-induced chemotaxis of THP-1 cells, a human monocytic leukemia cell line that shares many properties with human monocyte-derived macrophages.[28] Compound **1** inhibited chemotaxis with an IC$_{50}$ of

Table 1. Effect of Substitution on Ring A and Acylurea Linker

compd	R$_1$	R$_2$	R$_3$	R$_4$	chemotaxis IC$_{50}$ (μM)[a]
1	H	H	Cl	OH	3.9
2	H	H	Cl	H	1.6
3	H	H	Cl	Cl	1.5
4	H	H	CF$_3$	H	1.5
5	H	H	O^{i}Pr	H	1.0
6	H	H	Ph	H	>10
7	H	H	H	Ph	>10
8	Me	H	Cl	H	>10
9	Me	Me	Cl	H	>10

[a] Inhibition of hCCL2-induced chemotaxis of THP-1 cells. Cells were induced to migrate in response to hCCL2 in the presence of various concentrations of compound. The concentration that reduced migration by 50% (IC$_{50}$) is shown.

3.9 μM and showed no cytotoxicity (CC$_{50}$ > 50 μM) against this cell line.

Following the discovery of **1**, a medicinal chemistry program was launched to assess the effect of modifying each of the three structural components of the molecule, namely, ring A, the acylurea linker, and the bicyclic ring system B−C. Small lipophilic substituents (e.g., Cl, CF$_3$, O-^{i}Pr) on position 3 and/or position 4 of ring A were well tolerated and provided a 2- to 4-fold improvement in potency in the chemotaxis assay; larger groups (e.g., Ph) resulted in the loss of inhibitory activity, as did alkylation of the urea nitrogens (Table 1). Replacement of the acylurea linker by an acylguanidine (cf. **10**, Figure 3) or a conformationally rigid 1,2,4-oxadiazol-3-amine (cf. **11**) also suppressed activity, as did the transposition of the A and B−C rings (cf. **12**). This last observation suggested the existence of a unidirectional mode of binding of these molecules relative to the substituents on either side of the acylurea linker.

Replacement of the benzo[d][1,3]dioxole ring system B−C with different heterocycles led to the identification of the pyrazolo[3,4-b]pyridine derivative **13** (Figure 4) as a submicromolar inhibitor of CCL2-induced chemotaxis (IC$_{50}$ = 0.7 μM) with no cytotoxicity (CC$_{50}$ > 50 μM). Interestingly, **13** possesses structural features also present in other small-molecule CCR2 antagonists, specifically, a basic heterocyclic ring connected by a spacing moiety (the acylurea linker) to a lipophilic aromatic group.[29]

Examination of **13** in vivo revealed three hydroxylated metabolites, which were assigned as **14**, **15**, and **16** on the basis of LC−MS data (Figure 5).

With this information at hand, we focused our lead optimization efforts on introducing structural modifications to **13** that would prevent the formation of these phenolic metabolites. Different combinations of substituents at the 3- and/or 4-position of phenyl ring A were explored to preclude the formation of **14**. The most effective solution involved removal of the 4-F substituent and replacement of the electron-withdrawing 3-CF$_3$ group by an electron-donating group of similar lipophilicity, such as an isopropoxy. To prevent hydroxylation at the 6-position of the pyrazolopyridine ring leading to **15**, a salt-forming group was
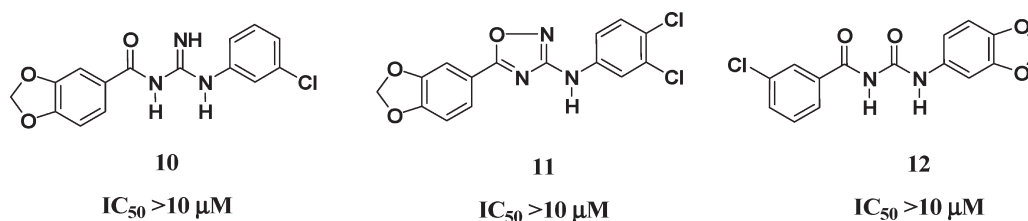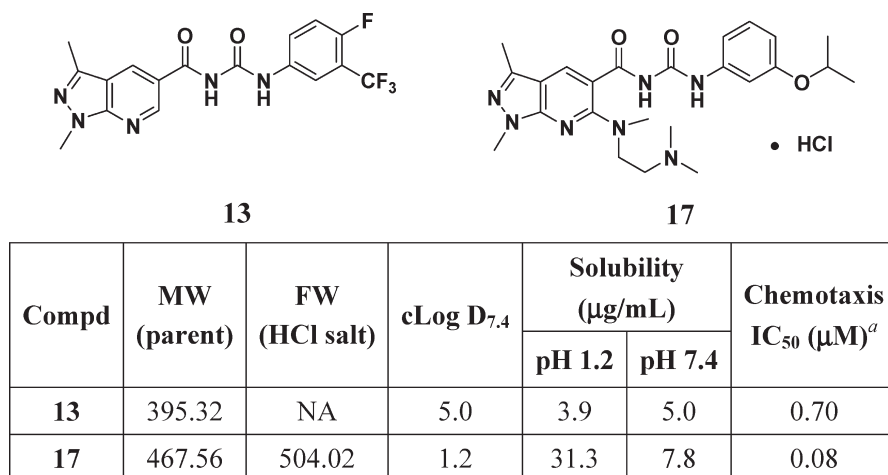
Figure 3. Effect of modifying the acylurea linker or transposing rings A and B—C.

Compd	MW (parent)	FW (HCl salt)	cLog $D_{7.4}$	Solubility (μg/mL) pH 1.2	pH 7.4	Chemotaxis IC$_{50}$ (μM)[a]
13	395.32	NA	5.0	3.9	5.0	0.70
17	467.56	504.02	1.2	31.3	7.8	0.08

[a] Inhibition of hCCL2-induced chemotaxis of THP-1 cells.

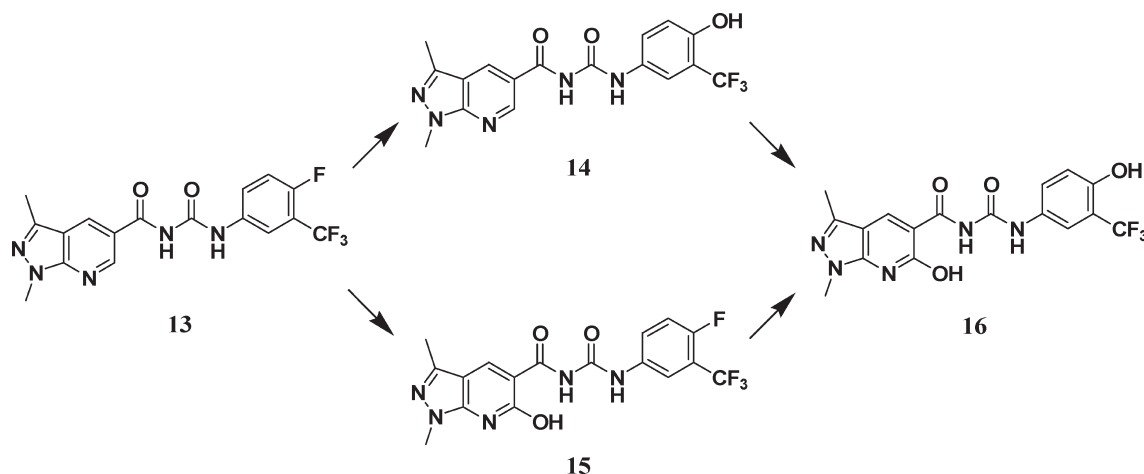**Figure 4.** Structure and properties of compounds **13** and **17**.

Figure 5. Metabolites of compound **13** in rat.

introduced at this position not only to block metabolic oxidation but also to increase the aqueous solubility of the resulting molecule. Among the several analogues prepared, **17** (Figure 4) showed improved solubility and a nearly 10-fold increase in chemotaxis inhibitory potency (IC$_{50}$ = 80 nM) relative to **13**.

■ CHEMISTRY

The aroyl- and heteroaroylphenylureas were synthesized by either of two methods depending on the commercial availability of the starting materials (Scheme 1). In method A, a carboxamide was converted into the corresponding acyl isocyanate by reaction with oxalyl chloride, and the acyl isocyanate was immediately reacted with an aniline to give the final acylurea. In method B, the carboxamide was reacted with an aryl isocyanate to afford the acylurea directly. In cases where the isocyanate was not commercially available, it was prepared by reaction of the corresponding aniline with triphosgene. The acylureas were isolated by precipitation from the reaction media and further purified by preparative HPLC or recrystallization.

Compound **17**, in particular, was prepared according to the sequence shown in Scheme 2. Commercially available 2,5-dimethyl-2H-pyrazol-3-ylamine, **18**, was converted into pyrazolo[3,4-b]

pyridine-5-carbonitrile **19** via a Vilsmeier–Haack reaction followed by condensation of the resulting aldehyde with ethyl cyanoacetate and intramolecular cyclization to form the bicyclic ring system. Treatment of **19** with phenylphosphonyl dichloride followed by N,N,N′-trimethylethane-1,2-diamine and subsequent hydrolysis of the nitrile group provided carboxamide **20**, which was then reacted with 3-isopropoxyphenyl isocyanate to afford **17** as the hydrochloride salt after treatment with HCl in dioxane.

■ IN VITRO PHARMACOLOGY

Chemotaxis. All new compounds were tested for their ability to inhibit hCCL2-induced migration of THP-1 cells. Briefly, the cells were incubated with different concentrations of compound in a modified Boyden chamber and induced to migrate in response to 12.5 nM hCCL2. The extent of cell migration was quantified by counting stained cells, and the concentration that reduced migration by 50% was reported as the IC50. Representative data are shown in Figure 6.

Selectivity. To assess the degree of selectivity toward CCL2/CCR2, representative compounds were tested for their ability to inhibit chemotaxis mediated by the binding of other chemokines to their cognate receptors. As shown in Table 2, compounds **13** and **17** were mostly selective for CCL2, as they did not significantly inhibit chemotaxis induced by CCL3 (MIP-1α), CCL5 (RANTES), CCL11 (eotaxin), CCL17 (TARC), or CXCL8 (IL-8). However, both compounds did inhibit chemotaxis of human peripheral blood mononuclear cells induced by CCL4 (MIP-1β), albeit with weaker potency. This chemokine

signals through CCR5, a receptor closely related to CCR2. It is worth noting that a number of small-molecule CCR2 antagonists reported in the literature also bind to CCR5 with a range of relative affinities.[30,31]

Receptor Binding Studies. Compounds **1** and **13** were evaluated for their ability to antagonize the binding of hCCL2 to CCR2 expressed in THP-1 or HEK293 cells. Surprisingly, despite their potent and fairly selective chemotaxis inhibitory activity, neither compound competed with the binding of ^{125}I-labeled CCL2 to the receptor (<10% inhibition of control-specific binding at 10 μM). This observation suggests the possibility that the compounds may be acting as noncompetitive allosteric inhibitors of CCR2, a mode of action that has been reported for other chemokine receptor antagonists.[32,33]

Compound **13** was also examined for its ability to bind to other chemokine receptors (CCR4 and CXCR1/2), as well as to the complement component 5a receptor (C5aR), all of which are also potent mediators of leukocyte migration during inflammation. As expected based on the chemotaxis data, the compound did not inhibit binding (<10% inhibition at 10 μM) of ^{125}I-CCL17 (TARC) to human recombinant CCR4 expressed in CHO-K1 cells or of ^{125}I-CXCL8 (IL-8) to CXCR1/2 expressed in human neutrophils or of ^{125}I-hC5a to hC5aR expressed in human recombinant CHO cells.

CCL2 Binding Studies. The possibility that the compounds were binding to CCL2 rather than to CCR2 was examined using two-dimensional heteronuclear shift correlation NMR spectroscopy. Compound **17** was incubated with isotopically labeled ^{15}N-CCL2 (ratio CCL2/compound = 1:1 and 2:1), and a two-dimensional ^{1}H–^{15}N heteronuclear single quantum coherence (HSQC) spectrum was recorded. No evidence of compound binding to CCL2 was observed.

Calcium Mobilization Studies. The binding of chemokines to their receptors is transduced into a variety of biochemical and physiological changes, including inhibition of cAMP synthesis, mobilization of calcium from intracellular pools into the cytosol, up-regulation of adhesion proteins, receptor desensitization and internalization, and cytoskeletal rearrangements leading to chemotaxis.[34] The molecular details of the chemokine–receptor interactions responsible for inducing signaling pathways that lead to each of these physiological changes are still being elucidated. Notwithstanding the complexity of these events, the rapid increase in cytosolic free calcium (Ca^{2+}) concentration upon CCR2 activation by CCL2 is frequently used as a functional assay for measuring the activity of CCR2 antagonists. Compound **1** was tested in this assay where it displayed a concentration-dependent inhibition of CCL2-stimulated calcium flux in THP-1 cells. However, this inhibition was weak and not significantly different from that of the vehicle control even at 50 μM (Figure 7).

Scheme 1. Preparation of Aroyl- and Heteroaroylphenylureas

Ar1 = Aryl or heteroaryl
Ar2 = Substituted phenyl
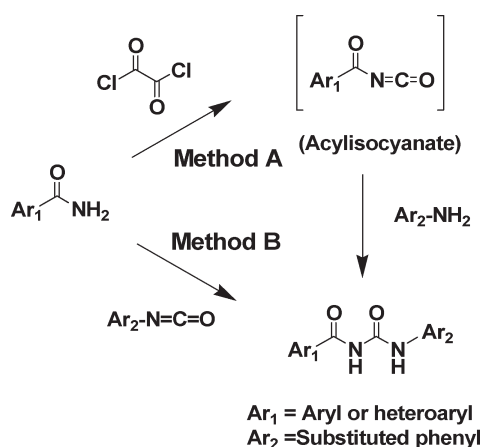
Scheme 2. Synthesis of Compound 17[a]
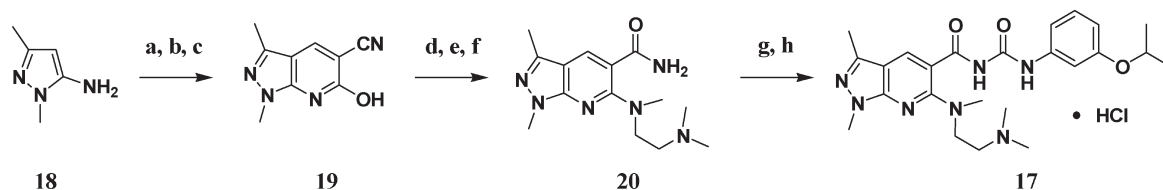
[a] Reagents: (a) DMF, POCl3; (b) NaOH, EtOH; (c) ethyl cyanoacetate; (d) PhPOCl2; (e) N,N,N′-trimethylethane-1,2-diamine, THF; (f) H2SO4; (g) 3-(Isopropoxy)phenylisocyanate, Et3N, toluene; (h) HCl, dioxane.

Species Specificity. A significant number of the CCR2 antagonists disclosed in the literature have been optimized for the human receptor and show little or no cross-reactivity to rodent CCR2, precluding their pharmacological evaluation in rodent models of inflammation. For this reason, we evaluated select compounds for their ability to inhibit chemotaxis mediated by mouse and/or rat CCL2. Although most compounds inhibited chemotaxis regardless of CCL2's origin, relative potencies varied from one compound to another. For example, **13** inhibited chemotaxis mediated by human and mouse CCL2 with similar potency, whereas **17** showed a significant difference in chemotaxis IC_{50} values between human and mouse or rat CCL2 (Table 3). In spite of this difference, **17** proved to be highly efficacious in rodent models of rheumatoid arthritis and multiple sclerosis (vide infra).

CYP450 Inhibition. Compound **17** was tested for inhibition of five major CYP450 isoenzymes at 1 and 100 μM. Very low ($\leq$11%) or no inhibition was observed at the lower concentration. At 100 μM, the compound was found to be a moderate inhibitor of CYP3A4, CYP2C9, and CYP2C19 and a stronger inhibitor of CYP2D6 (Table 4). The clinical relevance of these data with regard to potential drug—drug interaction, however, is considered to be low.

■ IN VIVO PHARMACOLOGY

Pharmacokinetics. Compound **17** was examined for oral bioavailability in rat. It exhibited a long apparent half-life after oral administration, suggesting that absorption may be a limiting factor (Figure 8). The extrapolated oral bioavailability, however, was quite good ($F = 60\%$).
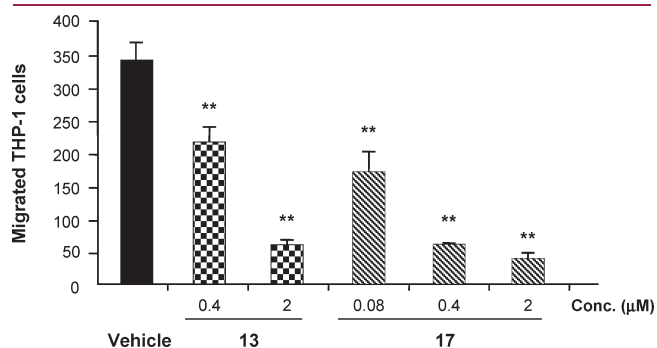
Figure 6. Inhibition of THP-1 cell chemotaxis by compounds **13** and **17**: *, $p < 0.05$; **, $p < 0.01$ (two-tailed t test).

Inhibition of Macrophage Recruitment. Thioglycollate-Induced Peritonitis Model. The thioglycollate-induced peritonitis model represents a rapid screen for anti-inflammatory activity in vivo. In this model, thioglycollate is injected in the peritoneal cavity of mice to induce local recruitment of leukocytes. Neutrophil accumulation usually reaches a peak at 6 h and declines rapidly, while the number of monocytes/macrophages gradually increases and reaches a peak at 72 h.[35] Several studies using CCR2 knockout or CCL2-deficient mice have demonstrated a selective reduction of monocyte influx in this model.[36−38] CCL2 knockout mice were specifically unable to recruit monocytes 72 h after intraperitoneal thioglycollate administration.[39] To ascertain whether our compounds were able to inhibit monocyte migration in vivo, we tested **13** in this model. Mice were injected with 3% Brewer's thioglycollate broth into the peritoneal cavity. Compound **13** was administered subcutaneously 3 h prior to and immediately after the injection of thioglycollate and then again 3 h after injection. An anti-CCL2 antibody was used as a positive control. Three days after the thioglycollate administration, the mice were sacrificed and the total number of elicited cells and MOMA-2 positive cells in the peritoneal cavity were analyzed by flow cytometry.[40] As shown in Table 5, compound **13** at a dose of 5 mg/kg significantly reduced the accumulation of total elicited cells and MOMA-2 positive cells in the peritoneal exudate. This result demonstrated that the in vitro chemotaxis inhibitory effect of **13** is also exhibited in vivo.
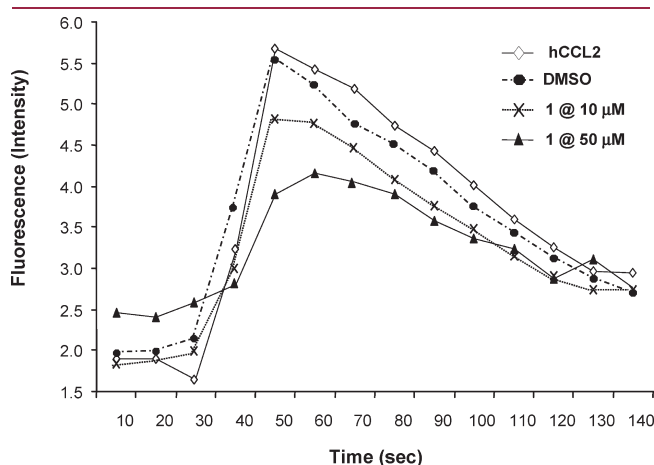
Figure 7. Effect of compound **1** on hCCL2-stimulated calcium flux in THP-1 cells. Inhibition achieved by increasing concentration of test compound was calculated as a percentage of the compound-free DMSO control.

Table 2. Inhibition of Chemotaxis Mediated by Different Chemokine-Receptor Systems

chemokine	chemokine receptor(s)	cell type	chemotaxis IC_{50} (μM) vs the indicated chemokine and cell type	
			13	**17**
CCL2	CCR2	THP-1	0.7	0.08
CCL2	CCR2	PBMC	NT	0.2
CCL3	CCR1, CCR5	PBMC	>10	>10
CCL4	CCR5	PBMC	2.9	0.4
CCL5	CCR1, CCR3, CCR5	PBMC	NT	>10
CCL11	CCR1, CCR3	eosinophil	NT	>10
CCL17	CCR4	CCR4-transfected THP-1	>10	>10
CXCL8	CXCR1, CXCR2	PMN	>10	>10

Table 3. Inhibition of Chemotaxis Mediated by Human, Mouse, and Rat CCL2[a]

compd	hCCL2 (THP-1 cells)	mCCL2 (mouse spleen cells)	rCCL2 (rat spleen cells)
13	0.70	1.4	NT
17	0.08	12.0	10.0

[a] Chemotaxis IC_{50} (μM) values vs the indicated chemokine and cell type: h = human; m = mouse; r = rat.

Table 4. CYP450 Inhibition by Compound 17

		% inhibition				
compd	concn (μM)	CYPA12	CYP3A4	CYP2C9	CYP2C19	CYP2D6
17	1	−12	4	11	−8	−5
	100	−2	49	36	34	73

Suppression of DTH Response. The delayed-type hypersensitivity (DTH) response is a well characterized model frequently used as an indicator of cell-mediated immune status.[41] The model is dependent upon both T helper 1 (Th1) driven responses and recruitment and chemotaxis to a local site. As a result, the DTH functional response may be influenced by disruption of Th1-driven, antigen-dependent T-cell development, or mobilization of sensitized T-cells to a local site. The model is usually performed by first injecting small quantities of an antigen during the sensitization (or immunization) phase and then again during the challenge (or inflammatory) phase. A hallmark response is elicited, which includes induration, swelling, and monocytic infiltration into the site of the lesion within 24−72 h. CCR2 knockout or CCL2-deficient mice have significant defects in both delayed-type hypersensitivity responses and production of Th1-type cytokines.[37,39] To determine the effect of **17** in the murine DTH reaction, mice were first immunized with sheep red blood cells (SRBC) and 4 days later challenged with SRBCs administered intradermally in their footpad. Vehicle or varying doses of **17** were given orally 1 h prior to and 2 h after challenge, and the footpad thickness was measured on day 5. As shown in Figure 9, treatment with **17** resulted in a dose-dependent suppression of footpad swelling.

Collagen-Induced Arthritis Model of Rheumatoid Arthritis. Compound **17** was evaluated prophylactically in the rat collagen-induced arthritis (CIA) model. CIA is an animal model of rheumatoid arthritis (RA) widely used to study disease pathogenesis and to test potential antiarthritic agents. Arthritis is normally induced in mice or rats by immunization with homologous or heterologous type II collagen in an adjuvant. Susceptibility to CIA is associated with major histocompatibility complex class II genes, and the development of arthritis is accompanied by a strong T- and B-cell response. The main pathological features of CIA include a proliferative synovitis with infiltration of polymorphonuclear and mononuclear cells, pannus formation, marked cartilage destruction associated with immune complex deposition on articular surfaces, bone resorption, and fibrosis. As in RA, proinflammatory cytokines such as tumor necrosis factor α (TNF-α) and interleukin-1 β (IL-1β) are highly expressed in the arthritic joints of mice and rats with CIA, and blockade of these cytokines results in a reduction of disease severity.[42]

Both CCL2 and CCR2 have been implicated in the pathogenesis of CIA in rats, with CCR2 reportedly having a dual role during initiation and progression of the disease. CCL2 concentrations in the joint lavages and CCL2 mRNA levels in the joint tissues both peak at approximately 2 weeks after immunization. Injection of a neutralizing monoclonal antibody (mAb) against rat CCL2 significantly decreased the number of exudate macrophages in the lesions and reduced swelling by 30% compared with controls.[43] Similarly, blockade of CCR2 with mAbs during the first 2 weeks after immunization markedly improved clinical signs and histological scores measuring leukocyte infiltration, synovial hyperplasia, and bone and cartilage erosion. CCR2 blockade from days 21 to 36, on the other hand, aggravated clinical and histological signs of arthritis and increased the humoral immune response against collagen.[44]

Lewis female rats were immunized on day 0 and then again on day 7 with bovine collagen type II. Vehicle, compound **17** (2, 10, or 30 mg/kg, b.i.d.), or methotrexate (MTX, 0.2 mg/kg, 3 × week) was given orally for 28 days starting on day 0 immediately after the first immunization. The degree of footpad swelling was measured on days 12, 14, 21, and 28 after immunization. As shown in Figure 10, treatment with **17** resulted in a dose-dependent inhibition of footpad swelling. On day 29, the animals were sacrificed and radiographs of the hind paws were taken to assess the extent of bone destruction. Radiological evaluation was performed by a blinded independent observer using an arbitrary scale (Figure 11). Treatment with **17** at 30 mg/kg b.i.d. significantly inhibited bone resorption in the joints of these animals (Figure 12).

The concentration of **17** in plasma, tarsal homogenates, and bone marrow (thigh bone) was measured 5 h after the last dosing on day 28 of the CIA study. As shown in Figure 13, compound **17** accumulated preferentially in the tarsal joints and bone marrow, where it reached concentrations well above its IC_{50} against rat CCL2.

Adjuvant-Induced Arthritis Model of Rheumatoid Arthritis. Compound **17** was also evaluated in the rat adjuvant-induced arthritis (AIA) model using a therapeutic dosing schedule. AIA is a form of (sub)chronic arthritis. Strains of rats have a varying genetic susceptibility to AIA, whereas mice generally are not susceptible. The disease is a T-cell-mediated autoimmune arthritis frequently used to study immunological aspects of RA and as a model for testing anti-inflammatory drugs.[45] Increased expression of CCL2 and CCR2 has been observed in the knee joints of rats with AIA, suggesting a role for this chemokine/receptor system in triggering the mechanisms involved in the pathogenesis of AIA.[46,47] Furthermore, postonset treatment of AIA-bearing rats with an inhibitor of endogenous CCL2 (P8A-CCL2) improved clinical signs of arthritis and histological scores measuring joint destruction, synovial lining, macrophage infiltration, and bone erosion.[48]

Following a typical protocol, Lewis female rats were immunized on day 0 by intradermal injection of Freund's complete adjuvant into the footpad of the right hind paw. Oral dosing with vehicle, compound **17** (10 or 30 mg/kg, b.i.d.), or methotrexate (MTX, 0.2 mg/kg, 3 × week) started on day 10, when macrophages had already begun to infiltrate the joint, and continued for an additional 18 days. Paw swelling was assessed by measuring the thickness of the footpad. Significant inhibition of footpad swelling was achieved with **17** at 30 mg/kg b.i.d. (Figure 14).

EAE Model of Multiple Sclerosis. Several studies have provided evidence that CCL2-dependent leukocyte chemotaxis
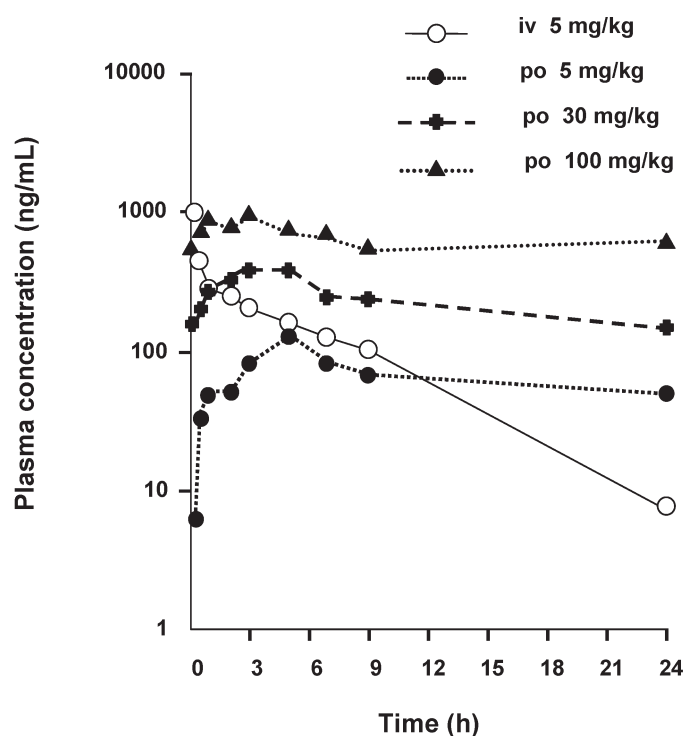
Route	Dose (mg/kg)	C_{max} (ng/mL)	t_{max} (h)	$t_{1/2}$ (h)	$AUC_{(0-24)}$ (h*ng/mL)	V_{dss} (L/kg)	CL (L/h/kg)	F (%)
i.v.	5	--	--	10	2691	9.9	1.9	--
p.o.	5	129	5	>24	(1618)	--	--	60
p.o.	30	383	3		(5568)			
p.o.	100	927	3		(15063)			

Figure 8. Pharmacokinetics of compound **17** after a single intravenous or oral dose to nonfasted rats. Because of the long half-life of the compound, AUC_{0-24} values are estimated.

Table 5. Inhibition of Macrophage Recruitment by Compound 13 in the Thioglycollate-Induced Peritonitis Model in Mice

treatment	dose (mg/kg)	cell number ($\times 10^6$)[a]	
		total cells	MOMA-2 positive cells
no treatment		2.1 ± 0.3**	1.2 ± 0.2**
vehicle		24.4 ± 1.1	18.5 ± 0.9
13	5	19.7 ± 1.6*	14.3 ± 1.2*
anti-CCL2 Ab	1	12.3 ± 1.8**	8.8 ± 1.2**

[a] Values are the mean ± SD: *, $p < 0.05$; **, $p < 0.01$ (two-tailed t test).

is a critically important event for the development of experimental autoimmune encephalomyelitis (EAE), a mouse model of chronic neuroinflammation resembling multiple sclerosis (MS).[49] Knockout mice lacking either CCL2 or CCR2 have been reported to be markedly resistant to developing EAE, although susceptibility to EAE in different mice strains lacking CCR2 has also been observed.[50−53] Treatment of EAE-bearing mice with an anti-CCL2 antibody or a small-molecule CCR2 antagonist, on the other hand, has been shown to reduce CNS macrophage accumulation and decrease the clinical severity of the disease.[54,55] Therefore, we chose EAE as a disease model to further evaluate the efficacy of compound **17**.

C57BL/6 mice were immunized subcutaneously with an encephalitogenic emulsion of the myelin oligodendrocyte glycoprotein-derived peptide MOG$_{33−55}$.[56,57] Starting on the day of the immunization (day 0), mice were given vehicle or **17**, once or twice a day orally, and were monitored daily for disease onset and severity of clinical symptoms. As shown in Table 6, treatment with compound **17** at 30 mg/kg b.i.d. significantly delayed the onset of EAE.

Neurological impairment was quantified on an arbitrary scale as follows: 0 = no detectable impairment; 1 = flaccid tail; 2 = hind
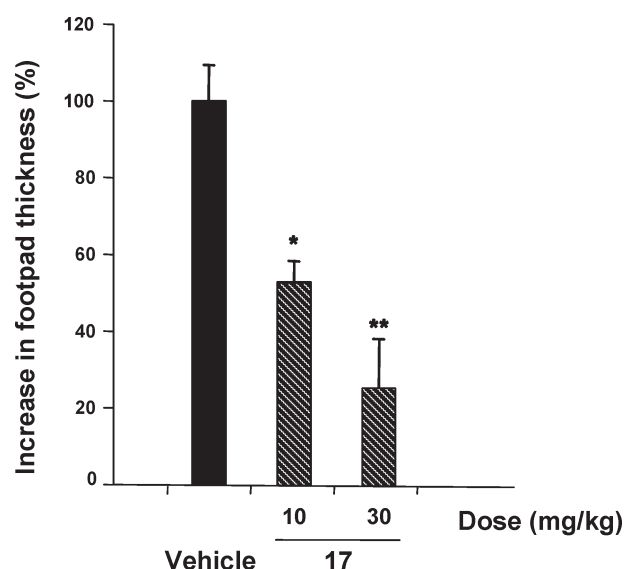
Figure 9. Effect of compound **17** on the DTH response in mice: *, $p < 0.05$; **, $p < 0.01$ (two-tailed t test).
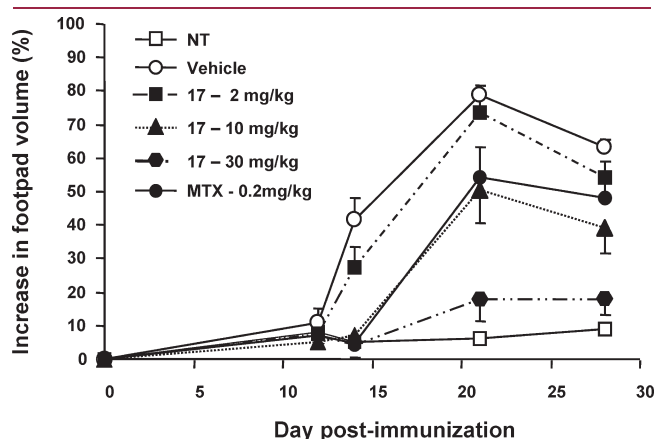

Figure 10. Effect of compound **17** on footpad swelling in the CIA prophylactic model. MTX = methotrexate.

limb weakness; 3 = hind limb paralysis; 4 = hind limb paralysis and ascending paralysis; 5 = moribund or deceased. Figure 15 shows the mean clinical score for the vehicle and the **17**-treated groups as a function of the number of days after immunization. Compound **17** ameliorated the symptoms of EAE in a dose-dependent manner and essentially produced a complete resolution of clinical symptoms at 30 mg/kg b.i.d.

Histological examination of brain, cerebellum, and spinal cord showed a significant decrease in inflammatory cell infiltrates following treatment with **17** (Figure 16).

■ TOXICOLOGY STUDIES

Compound **17** was examined for overt toxicity in 6-week-old male ICR mice after single (acute) and repeated (2-week) oral dosing. In the acute study, no signs of toxicity were observed at doses up to 100 mg/kg. Hypoactivity was observed at 500 mg/kg, whereas CNS excitation (tonic convulsions, Straub tail) and increased feeding behavior were observed at 1000 mg/kg.

In the 2-week repeated-dose study, mice were dosed orally once a day for 14 days with vehicle or with 30, 100, or 300 mg/kg of compound **17**. All the animals survived the study, and no abnormal behavior or significant body weight changes were observed at any of the doses tested. Elevated liver enzymes (AST and ALT) were observed at the highest dose tested (300 mg/kg). Histological examination showed signs of liver and kidney toxicity (i.e., vacuolar degeneration) at this dose.

■ SUMMARY AND CONCLUSIONS

Through the application of TRAP, we discovered a new class of heteroaroylphenylureas that inhibit chemotaxis of monocytes/macrophages induced by the chemokine CCL2. Medicinal chemistry optimization of the initial lead for potency and metabolic stability resulted in the identification of **17**, a potent small-molecule inhibitor of human CCL2-induced chemotaxis. This inhibition was selective for CCL2, since **17** did not inhibit chemotaxis induced by other chemokines except for CCL4, which was inhibited with a >5-fold lower potency. In spite of this selectivity, the new class of compounds did not compete with the binding of radiolabeled CCL2 to the CCR2 receptor nor did they significantly inhibit biochemical processes (e.g., Ca^{2+} mobilization) that are triggered upon CCR2 activation by CCL2. The in vivo pharmacologic profile of these compounds, however,
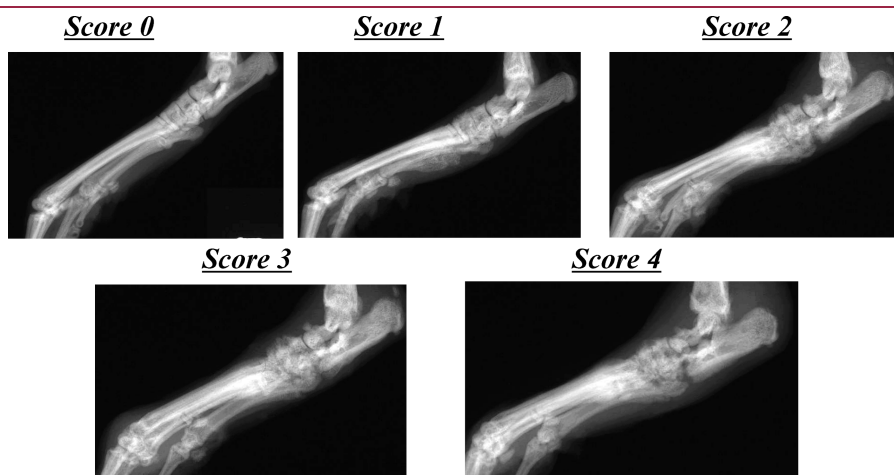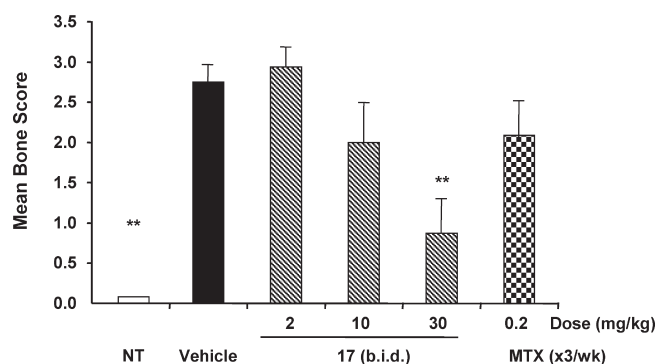

Figure 11. Bone destruction scoring in the CIA model. Scores are as follows: 0 = normal; 1 = slight damage; 2 = mild damage; 3 = obvious damage; 4 = marked destruction.

Figure 12. Effect of compound **17** on bone resorption in the CIA prophylactic model. Radiographs of both hind paws were taken and bone condition graded from 0 = normal to 4 = marked destruction. The average of both legs was calculated and assigned the score shown. NT = no treatment. MTX = methotrexate. $*$, $p < 0.05$; $**$, $p < 0.01$ (two-tailed t test).
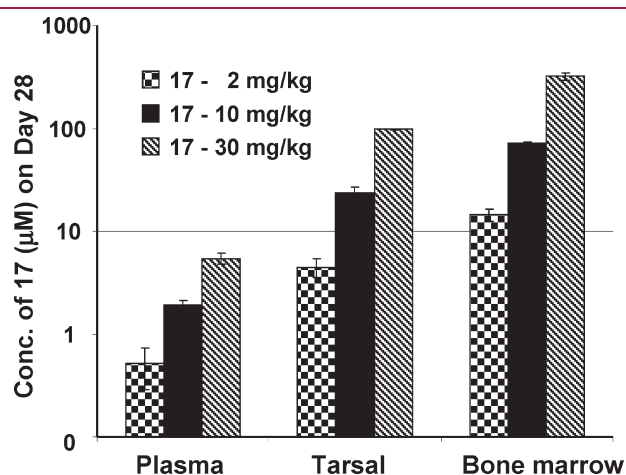
Figure 13. Concentration of compound **17** (logarithmic scale) in plasma, tarsal joints, and bone marrow on day 28 of the CIA prophylactic model study.

closely resembles the CCR2 or CCL2 knockout phenotypes in classical models of macrophage trafficking and parallels that of other selective CCR2 antagonists described in the literature.[55] Indeed, the reduction of monocyte/macrophage infiltration in the thioglycolate-induced peritonitis model observed with **13** and the impaired delayed-type hypersensitivity response seen with **17** mirror effects reported for CCR2 or CCL2 knockout mice, suggesting that the compounds block the pharmacological actions mediated by this chemokine/receptor interaction. Interestingly, a previous DTH study using CCL2 knockout mice showed a reduction in the number of F4/80-positive macrophages in the ears of mice undergoing the DTH reaction, but the swelling response was normal.[39] The result of our DTH study with **17** has more similarities with that reported for a small-molecule CCR2 antagonist which reduced not only monocyte influx but also swelling.[55] It is well established that macrophages accumulate at the DTH site and become activated through the CD4 Th1 cell−cytokine−macrophage axis, producing various proinflammatory cytokines and chemotactic factors that lead to local inflammation.

The efficacy observed in the rat CIA model following prophylactic dosing of **17** is of particular relevance given that different outcomes were reported in this disease model when different methods and schedules of CCL2 inhibition were used. Blockade of CCR2 with an anti-CCR2 antibody before the onset of CIA resulted in disease amelioration. In contrast, blockade with the same antibody after disease onset (i.e., therapeutic administration) markedly aggravated the clinical and histological signs of arthritis.[44] Similarly, CCL2(9−76), a CCL2 antagonist that blocks CCL2 binding to CCR2, prevented the spontaneous onset of arthritis in the MRL-*lpr* mouse model but was less effective when given only after the disease had already developed.[58] Compound **17** was also efficacious in the EAE mouse model of MS when administered prophylactically, that is, under conditions that replicate previous studies using CCR2 knockout or CCL2-null mice.[50−52] On the other hand, therapeutic dosing of **17** in the AIA model resulted in significant reduction of footpad swelling, in agreement with the effects observed with other small-molecule CCR2 antagonists when dosed after the onset of the disease.[55] These observations suggest
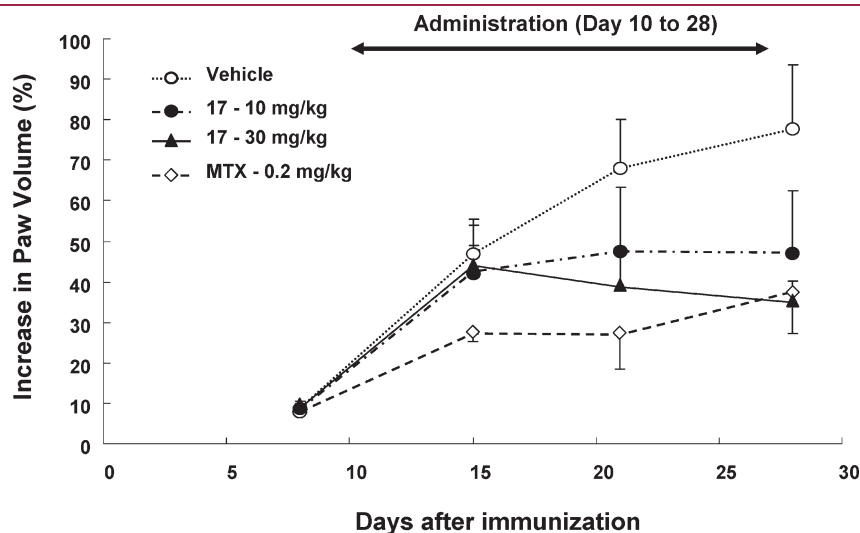
Figure 14. Effect of compound **17** on footpad swelling in the AIA therapeutic model. MTX = methotrexate.

that the outcome of inhibiting CCL2 or blocking CCR2 depends on the disease model, the nature of the inhibitor, and the timing of its administration.

Although we cannot rule out other mechanisms of action to explain the in vitro and in vivo pharmacologic profile of compounds such as **17**, the data presented herein support the hypothesis that these novel acylureas are antagonists of CCL2/CCR2 signaling and that they exert this action by binding to the receptor in an allosteric manner. Indeed, it has been shown that specific features of CCL2 can induce different conformations in CCR2 that are coupled to separate postreceptor signaling pathways. For example, certain mutations of surface-exposed CCL2 residues provided peptides that were agonists of pathways involving inhibition of cAMP synthesis and Ca^{2+} mobilization but antagonists of chemotaxis. These results demonstrate that the former two events are not sufficient to drive chemotaxis and that different ligands may be able to trap CCR2 in conformations that are unable to stimulate the pathways required for chemotaxis.[59] On the other hand, site-directed mutagenesis of CCR2 provided mutants with normal CCL2 binding but that were unable to elicit Ca^{2+} mobilization or inhibit adenylate cyclase at any CCL2 concentration. Some of these mutants, however, showed lamellipodia formation and were capable of inducing chemotaxis.[60] These examples illustrate the observation that most classic GPCR antagonists bind to the receptor's orthosteric site, that is, the site recognized by the endogenous agonist. However, it has become evident that GPCRs possess additional, extracellular, allosteric binding sites that can be recognized by a variety of small-molecule ligands. Allosteric modulators may even offer certain advantages over classic orthosteric ligands as therapeutic agents, including the potential for greater GPCR-subtype selectivity and safety.[61,62]

Several of the CCR2 antagonists reported in the literature lack rodent cross-reactivity, precluding their pharmacological evaluation in animal models of inflammation. Compound **17** proved to be a more potent inhibitor of chemotaxis induced by human CCL2 than by mouse or rat CCL2, but it was nonetheless efficacious in rodent models of arthritis and multiple sclerosis, most likely because of accumulation at the sites of inflammation. We can only speculate that, based on the chemotaxis data, it should be even more efficacious in man.

■ EXPERIMENTAL SECTION

General. All reactions were performed under an atmosphere of dry nitrogen. Commercial reagents were used without further purification. All final compounds were purified by preparative HPLC on a Varian PrepStar SD-1 system or by recrystallization from the indicated solvent. Final purity was determined by RP-HPLC analysis on a Varian Prostar 210 system using a Microsorb R0089200C5 column (250 mm × 4.6 mm, 3.5 μm), linear gradient elution with H_2O/MeCN containing 0.05% TFA, and UV detection at 254 nm. Purity and retention time [e.g., HPLC: t_R = 14.6 min (97% purity)] are given for each compound. Unless otherwise noted, all tested compounds had ≥95% purity. Molecular parent ion identity was determined by tandem LC−MS analysis on an Agilent 1100 LC/MSD instrument using a Zorbax Eclipse XDB-C8 column (2.1 mm × 50 mm, 3.5 μm), linear gradient elution with 10 mM aqueous ammonium acetate/MeCN containing 0.1% AcOH, UV detection at 254 nm, and atmospheric-pressure electrospray ionization (ESI) in either a negative (−) or positive (+) mode. ^{1}H NMR spectra were recorded at 400 MHz on a Varian Mercury-400 spectrometer; chemical shifts (δ) are reported in ppm downfield from internal tetramethylsilane (TMS) and coupling constants (J) in hertz (Hz).

The synthesis of representative compounds is given below.

1-(Benzo[*d*][1,3]dioxole-6-carbonyl)-3-(3-chloro-4-hydroxyphenyl)urea (1). Aqueous ammonium hydroxide (28−30% ammonia, 30 mL) was added dropwise to ice-cooled piperonyloyl chloride

Table 6. Effect of Compound 17 on the Development of Acute EAE

treatment	dose (mg/kg)	day of disease onset[a]
vehicle		17.3 ± 1.6
17	30 (b.i.d.)	32.7 ± 11.1*

[a] Values are the mean ± SD: *, $p < 0.05$ (two-tailed t test with unequal variance).
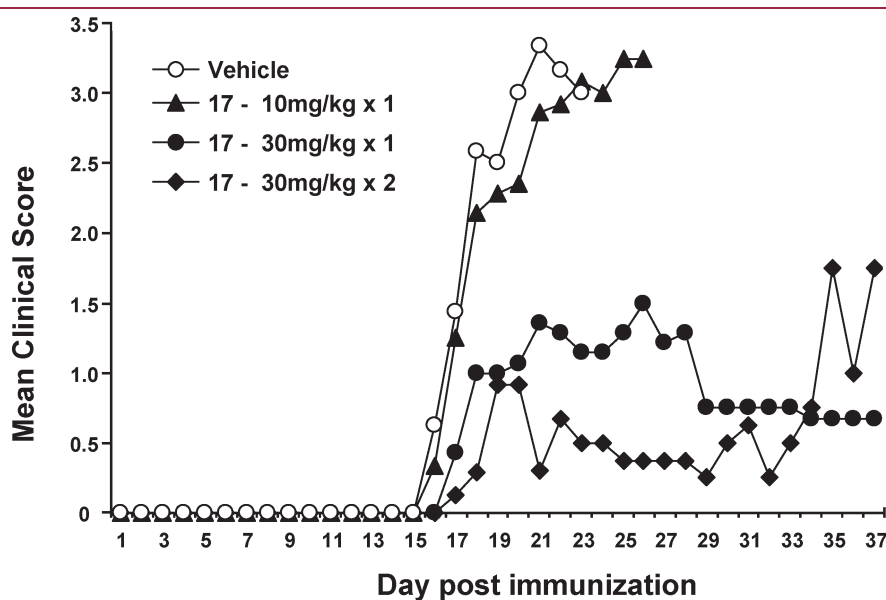
Figure 15. Effect of compound **17** on the clinical symptoms of acute EAE. Animals in the vehicle and **17** 10 mg/kg group were sacrificed on days 22 and 26, respectively, because of severe EAE.
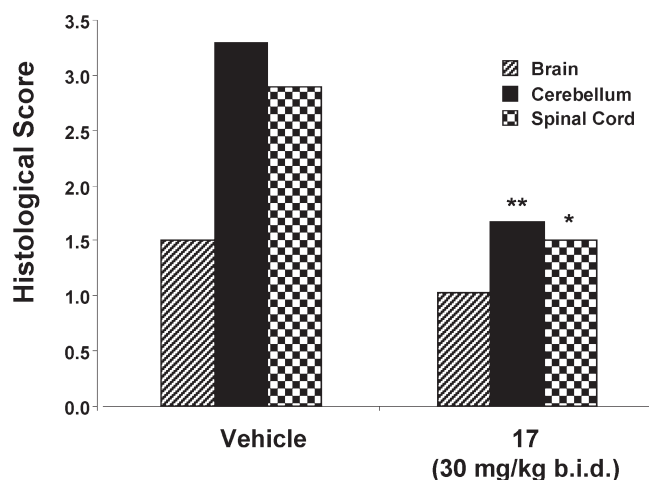
Figure 16. Effect of compound **17** on cellular infiltrates following acute EAE. Histological scores are as follows: 0 = no inflammation; 1 = very small cellular infiltrate in the perivascular areas and meninges; 2 = mild cellular infiltrate; 3 = moderate cellular infiltrate; 4 = severe cellular infiltrate; 5 = very large and extensive cellular infiltrate. $*$, $p < 0.05$; $**$, $p < 0.01$ (two-tailed t test).

(3.02 g, 16.36 mmol). The ice bath was removed, and the mixture was stirred at room temperature for 1 h. The resulting solid was collected by filtration, washed with water, and dried under high vacuum to yield benzo$[d]$1,3-dioxolene-5-carboxamide as a white powder. A portion of this material (0.199 g, 1.20 mmol) was suspended in anhydrous CH_2Cl_2 (6 mL) and treated with a 2 M solution of oxalyl chloride in CH_2Cl_2 (0.91 mL, 1.82 mmol). The mixture was heated at gentle reflux for 16 h and then cooled to room temperature. The solvent was removed under reduced pressure to give benzo$[d][1,3]$dioxole-5-carbonyl isocyanate, which was immediately dissolved in anhydrous THF and added to an ice-cooled solution of 4-amino-2-chlorophenol (0.174 g, 1.21 mmol) in anhydrous THF (2 mL). The ice bath was removed, and the mixture was stirred at room temperature for 2 h. The resulting solid was collected by filtration, washed with CH_2Cl_2, and dried under high vacuum to afford 0.183 g (46% yield) of **1** as a white powder. HPLC: t_R = 14.6 min (97% purity). MS ESI$^{(-)}$ = 333** (M − H). ^{1}H NMR (DMSO-d_6): δ 6.15 (s, 2H), 6.94 (d, 1H, J = 8.8 Hz), 7.06 (d, 1H, J = 8.2 Hz), 7.23 (d, 1H, J = 8.8 Hz), 7.64 (m, 2H), 10.02 (s, 1H), 10.68 (s, 1H), 10.82 (s, 1H).

Compounds **2**−**7** were prepared following a similar procedure.

1-(Benzo[d][1,3]dioxole-6-carbonyl)-3-(3-chlorophenyl) urea (2). White powder (38% yield). HPLC: t_R = 17.4 min (95% purity). MS ESI$^{(-)}$ = 317 (M − H). ^{1}H NMR (DMSO-d_6) δ: 6.16 (s, 2H), 7.06 (d, 1H, J = 8.2 Hz), 7.15 (d, 1H, J = 7.8 Hz), 7.35 (t, 1H, J = 8.0 Hz), 7.44 (d, 1H, J = 8.3 Hz), 7.59 (d, 1H, J = 1.6 Hz), 7.67 (d, 1H, J = 8.2 Hz), 7.83 (d, 1H, J = 2.0 Hz), 10.93 (s, 1H), 10.95 (s, 1H).

1-(Benzo[d][1,3]dioxole-6-carbonyl)-3-(3,4-dichlorophenyl) urea (3). White solid (41% yield). HPLC: t_R = 18.5 min (96% purity). MS ESI$^{(-)}$ = 351 (M − H). ^{1}H NMR (DMSO-d_6) δ: 6.16 (s, 2H), 7.07 (d, 1H, J = 7.8 Hz), 7.59 (t, 3H, J = 8.1 Hz), 7.68 (d, 1H, J = 7.9 Hz), 8.01 (s, 1H,), 10.96 (s, 1H), 10.97 (s, 1H).

1-(Benzo[d][1,3]dioxole-6-carbonyl)-3-(3-(trifluoromethyl) phenyl)urea (4). White solid (88% yield). HPLC: t_R = 16.3 min (98% purity). MS ESI$^{(+)}$ = 353 (M + H). ^{1}H NMR (DMSO-d_6) δ: 6.15 (s, 2H), 7.06 (d, 1H, J = 8.2 Hz), 7.44 (d, 1H, J = 7.3 Hz), 7.59 (m, 2H), 7.69 (d, 1H, J = 8.2 Hz), 7.78 (d, 1H, J = 7.7 Hz), 8.01 (s, 1H,), 10.94 (s, 1H), 11.05 (s, 1H).

1-(Benzo[d][1,3]dioxole-6-carbonyl)-3-(3-isopropoxyphenyl) urea (5). White solid (64% yield). HPLC: t_R = 16.7 min (99% purity). MS ESI$^{(-)}$ = 341 (M − H). ^{1}H NMR (DMSO-d_6) δ: 1.27 (d, 6H, J = 6.0 Hz),

4.60 (q, 1H, J = 6.0 Hz), 6.16 (s, 2H), 6.66 (d, 1H, J = 8.0 Hz), 7.05 (m, 2H), 7.22 (m, 2H), 7.59 (s, 1H), 7.68 (d, 1H, J = 8.2 Hz), 10.82 (s, 2H).

1-(Benzo[d][1,3]dioxole-6-carbonyl)-3-(3-phenylphenyl) urea (6). White solid (39% yield). HPLC: t_R = 17.6 min (98% purity). MS ESI$^{(-)}$ = 359 (M − H). ^{1}H NMR (DMSO-d_6) δ: 6.16 (s, 2H), 7.07 (d, 1H, J = 8.2 Hz), 7.14 (m, 2H), 7.49 (m, 3H,), 7.61 (s, 2H), 7.68 (m, 3H), 7.85 (s, 1H,), 10.86 (s, 1H), 10.96 (s, 1H).

1-(Benzo[d][1,3]dioxole-6-carbonyl)-3-(4-phenylphenyl) urea (7). White solid (80% yield). HPLC: t_R = 18.2 min (96% purity). MS ESI$^{(-)}$ = 359 (M − H). ^{1}H NMR (DMSO-d_6) δ: 6.16 (s, 2H), 7.07 (d, 1H, J = 8.2 Hz), 7.34 (t, 1H, J = 7.3 Hz), 7.46 (t, 2H, J = 7.8 Hz), 7.61 (s, 2H), 7.68 (m, 6H,), 10.89 (s, 1H), 10.94 (s, 1H).

1-(Benzo[d][1,3]dioxole-6-carbonyl)-3-(3-chlorophenyl)-1-methylurea (8). Lithium bis(trimethylsilyl)amide (0.38 mL of 1 M solution in THF) was added to a solution of **2** (0.10 g, 0.31 mmol) in DMF (5 mL), and the mixture was stirred for 30 min. Methyl iodide (69 μL, 1.1 mmol) was added, and the resulting solution was stirred at room temperature for an additional 4 h. Water (15 mL) was added, and the solution was filtered. The filtrate was collected, and the solvents were removed in vacuo. The resulting solid was triturated with water (30 mL), filtered, and dried under high vacuum to give **8** (16 mg, 16% yield). HPLC: t_R = 17.0 min (85% purity). MS ESI$^{(-)}$ = 331 (M − H). ^{1}H NMR (DMSO-d_6) δ: 3.32 (s, 3H), 6.07 (s, 2H), 6.90 (d, 1H, J = 8.1 Hz), 7.01 (s, 1H), 7.09 (d, 1H, J = 8.1 Hz), 7.24 (m, 2H), 7.32 (m, 1H), 7.73 (s, 1H), 11.41 (s, 1H).

1-(Benzo[d][1,3]dioxole-6-carbonyl)-3-(3-chlorophenyl)-1,3-dimethylurea (9). A solution of **2** (0.098 g, 0.307 mmol) in DMF (5 mL) was treated with sodium hydride (0.025 g, 0.625 mmol). and the mixture was stirred at room temperature for 30 min. Methyl iodide (39 μL, 0.626 mmol) was added and the resulting solution was stirred for an additional 3 h. The reaction was quenched with water (50 mL), and the mixture was extracted with CH_2Cl_2 (3 × 50 mL). The organic layers were combined, washed with water, dried over anhydrous $MgSO_4$, filtered, and concentrated under reduced pressure. The residue was chromatographed on silica gel (1:1 EtOAc/Hex) to give **9** (13 mg) as a colorless oil. HPLC: t_R = 14.9 min (97% purity). MS ESI$^{(+)}$ = 347 (M + H). ^{1}H NMR (DMSO-d_6) δ: 3.20 (s, 3H), 3.30 (s, 3H), 6.04 (s, 2H), 6.41 (s, 1H), 6.64 (d, 1H, J = 7.5 Hz), 6.69 (s, 1H), 6.77 (d, 1H, J = 8.2 Hz), 6.89 (d, 1H, J = 7.8 Hz), 7.22 (m, 2H).

1-(Benzo[d][1,3]dioxole-6-carbonyl)-3-(3-chlorophenyl) guanidine (10). Cyanamide (100 mg, 2.38 mmol) was dissolved in water (1 mL) and treated with piperonyl chloride (440 mg, 2.38 mmol). Aqueous NaOH (190 μL of a 12.5 N solution) was added, and the mixture was stirred for 2 h. 3-Chloroaniline (288 mg, 240 mmol) was added, and the pH of the solution was adjusted to pH 3 by addition of concentrated HCl. The mixture was diluted with water (5 mL), refluxed for 1 h, and then cooled to room temperature. The resulting solid was collected by filtration, dissolved in 30% aqueous NaOH (1 mL), and the solution was diluted with water (50 mL). The precipitated solid was filtered and dried under high vacuum to afford **10** as a white solid (106 mg, 14% yield). HPLC: t_R = 3.04 min (90% purity). MS ESI$^{(-)}$ = 316 (M − H). ^{1}H NMR (DMSO-d_6) δ: 6.09 (s, 2H), 6.95 (d, 1H, J = 8.1 Hz), 7.14 (d, 1H, J = 7.2 Hz), 7.36 (m, 2H), 7.53 (s, 1H), 7.69 (d, 1H, J = 8.2 Hz), 7.91 (s, 1H), 9.31 (s, 1H).

5-(Benzo[d][1,3]dioxol-5-yl)-N-(3,4-dichlorophenyl)-1,2,4-oxadiazol-3-amine (11). Cyanamide (82 mg, 1.95 mmol) was dissolved in water (1 mL) and treated with piperonyl chloride (369 mg, 1.95 mmol). Aqueous sodium hydroxide (160 μL of a 12.5 N solution) was added, and the mixture was stirred for 2 h. 3,4-Dichloroaniline (290 mg, 1.79 mmol) was added, and the pH of the solution adjusted to pH 3 by addition of concentrated HCl. The mixture was diluted with water (5 mL), refluxed for 1 h, and then cooled to room temperature. The resulting solid was collected by filtration, dissolved in 30% aqueous NaOH (1 mL) and the solution diluted with water (50 mL). The

precipitated solid was collected by filtration and dried under high vacuum. This solid was dissolved in 3:1 CH_2Cl_2/MeOH (4 mL) and the solution treated with 13% NaOCl (4 mL). The resulting biphasic solution was stirred at room temperature for 2 h. The aqueous layer was discarded, and the organic layer was treated with Na_2SO_3 (50 mg in 2 mL water) and methanol (5 mL). The resulting solution was refluxed for 16 h. The solvents were removed under reduced pressure and the residue was chromatographed on silica gel (1:1 EtOAc/Hex) to give 11 (16 mg) as a white solid. HPLC: t_R = 9.25 min (97% purity). MS ESI$^{(-)}$ = 348 (M − H). ^{1}H NMR (DMSO-d_6) δ: 6.20 (s, 2H), 7.17 (d, 1H, J = 8.2 Hz), 7.45 (d, 1H, J = 8.8 Hz), 7.50 (s, 1H), 7.58 (d, 1H, J = 8.9 Hz), 7.66 (d, 1H, J = 8.2 Hz), 7.75 (s, 1H), 10.40 (s, 1H).

1-(Benzo[d][1,3]dioxol-5-yl)-3-(3-chlorobenzoyl)urea (12). To a solution of 3,4-(methylene)dioxyaniline (82.6 mg, 0.60 mmol) in THF (2 mL) was added 3-chlorobenzoyl isocyanate (1 mL of a 0.60 M solution in THF). The solution was stirred at room temperature for 1 h. The precipitated solid was collected by filtration, washed with CH_2Cl_2, and dried under high vacuum to afford 12 (85.0 mg, 44% yield) as a white solid. HPLC: t_R = 16.5 min (88% purity). MS ESI$^{(-)}$ = 317 (M − H). ^{1}H NMR (DMSO-d_6) δ: 6.02 (s, 2H), 6.98 (m, 2H), 7.28 (s, 1H), 7.57 (t, 1H, J = 7.9 Hz), 7.73 (d, 1H, J = 9.0 Hz), 7.95 (d, 1H, J = 7.8 Hz), 8.05 (s, 1H), 10.56 (s, 1H), 11.08 (s, 1H).

1-(1,3-Dimethyl-1H-pyrazolo[3,4-b]pyridine-5-carbonyl)-3-(4-fluoro-3-(trifluoromethyl)phenyl)urea (13). 4-Chloro-1,3-dimethylpyrazolo[5,4-b]pyridine-5-carboxamide (3.5 g, 18.4 mmol) was dissolved in hot toluene (30 mL) and azeotroped for 1 h. The solution was allowed to cool to room temperature and treated with 4-fluoro-3-(trifluoromethyl)phenyl isocyanate (4.6 g, 22.1 mmol). The mixture was refluxed for 16 h and then cooled to room temperature. The precipitated solid was filtered, washed with MeOH, and dried under high vacuum to give 13 (3.6 g, 49% yield) as a white solid. HPLC: t_R = 16.2 min (99% purity). MS ESI$^{(-)}$ = 394 (M − H). ^{1}H NMR (DMSO-d_6) δ: 2.55 (s, 3H), 4.01 (s, 3H), 7.51 (t, 1H, J = 9.7 Hz), 7.90 (m, 1H), 8.12 (d, 1H, J = 6.3 Hz), 8.90 (s, 1H), 9.08 (s, 1H), 10.93 (s, 1H), 11.25 (s, 1H).

1-(6-((2-(Dimethylamino)ethyl)(methyl)amino)-1,3-dimethyl-1H-pyrazolo[3,4-b]pyridine-5-carbonyl)-3-(3-isopropoxyphenyl)urea Hydrochloride (17). A solution of 5-amino-1,3-dimethylpyrazole-4-carbaldehyde (6.15 g) in ethyl cyanoacetate (10 mL) was stirred at 185 °C for 3 h. The mixture was allowed to cool to room temperature, and the precipitated solid was filtered, washed with EtOAc, and dried under high vacuum to give 6-hydroxy-1,3-dimethylpyrazolo[5,4-b]pyridin-5-carbonitrile as a white powder. A portion of this material (2.18 g) was dissolved in phenylphosphonic dichloride (10 mL) and stirred at 150 °C for 17 h. The solution was cooled to room temperature and poured into water. The mixture was extracted with EtOAc. The organic layer was decanted, washed with saturated $NaHCO_3$ solution, dried over anhydrous Na_2SO_4, and filtered. The solvent was removed under reduced pressure to give a white solid. This material (2.16 g) was dissolved in THF (50 mL) and treated with N,N,N'-trimethylethane-1,2-diamine (10.6 mL). The mixture was heated at reflux for 20 h, cooled to room temperature, and extracted with EtOAc. The organic extracts were dried over anhydrous Na_2SO_4, filtered, and concentrated under reduced pressure to afford 6-{[2-(dimethylamino)ethyl]methylamino}-1,3-dimethylpyrazolo[5,4-b]pyridine-5-carbonitrile as a brown oil. This material (2.96 g) was dissolved in concentrated H_2SO_4 (10 mL), and the solution was stirred at 60 °C for 15 h. The mixture was then neutralized with saturated $NaHCO_3$ solution and extracted with CH_2Cl_2. The extracts were washed with NaCl solution, dried over Na_2SO_4, filtered, and concentrated under reduced pressure. The residue was purified by recrystallization from EtOAc−hexanes to give 6-{[2-(dimethylamino)ethyl]methylamino}-1,3-dimethylpyrazolo[5,4-b]pyridine-5-carboxamide as a white solid. A portion of this material (2.0 g, 6.8 mmol) was dissolved in hot toluene (20 mL) and azeotroped for 2 h. The solution was cooled to room temperature and treated with 3-isopropoxyphenyl isocyanate (1.7 g, 9.6 mmol). The mixture was refluxed

for 16 h and then cooled to room temperature. The solvent was removed under reduced pressure, and the residue was taken up in THF (100 mL) and treated with HCl (4 N in dioxane, 7 mL). The resulting solid was filtered, dried under high vacuum, and then recrystallized from MeCN to give 17 (2.55 g, 74% yield) as a white solid. HPLC: t_R = 10.5 min (99% purity). MS ESI$^{(-)}$ = 466 (M − H). ^{1}H NMR (DMSO-d_6) δ: 1.27 (d, 6H, J = 6.0 Hz), 2.41 (s, 3H), 2.53 (t, 2H, J = 6.4 Hz), 2.83 (s, 6H), 2.98 (s, 3H), 3.82 (s, 3H), 3.92 (t, 2H, J = 6.4 Hz), 4.60 (q, 1H, J = 6.0 Hz), 6.68 (m, 1H), 7.05 (m, 1H), 7.22 (m, 2H), 8.24 (s, 1H), 10.58 (s, 1H), 11.09 (s, 1H).

Biological Assays and Procedures. *Chemotaxis Assay.* Cell migration experiments were performed in a 48-well modified Boyden microchemotaxis chamber with a 5 μm pore size PVP-coated polycarbonate filter membrane (Neuro Probe Inc., Cabin John, MD). Compounds were prepared as 10 mM stock solution in DMSO and serially diluted with medium. THP-1 cells were washed with RPMI 1640 medium supplemented with 0.5% (w/v) bovine serum albumin (BSA) and 25 mM HEPES, pH 7.4, and suspended at a density of 4×10^6 cells/mL in the same medium. A 150 μL aliquot of this suspension was treated with an equal volume of test compound solution and the mixture incubated at 37 °C for 15 min. The lower chamber was loaded with 26 μL of a 2.5 nM solution of hCCL2 (PeproTech) in medium. The filter membrane was placed over the lower chamber, followed by a silicone rubber gasket and the upper chamber. A 50 μL aliquot of the THP-1 cell suspension containing the test compound was added to the upper chamber and the assembly incubated in a 5% CO_2 atmosphere at 37 °C for 2 h. The chamber was then disassembled, and the cells remaining on the upper surface of the filter were scraped off with a rubber scraper. The filter was fixed with methanol, stained with Diff-Quik solution, and mounted on a glass slide. The cells that had migrated across the filter onto the lower surface were then counted by microscopic observation. Chemotaxis studies using other chemokines and cell types were performed similarly.

Receptor Binding Assay. In vitro radioligand receptor binding assays were performed by Cerep (Poitiers, France; CCR2 ref no. 0362; C5a ref no. 0042) and Ricerca (formerly MDS Pharma Services, Taipei, Taiwan; CCR4 catalog no. 217660; CXCR1/2 - IL-8 nonselective catalog no. 244300).

Binding to CCL2 Studies. Compound 17 was incubated with isotopically labeled ^{15}N-CCL2 (250 μM) in either a 1:1 or a 1:2 CCL2-to-compound ratio, and the 2D ^{1}H/^{15}N shift correlation NMR spectrum (HSQC spectrum) was recorded.

Calcium Mobilization Assay. Intracellular calcium flux was measured as the increase in fluorescence emitted by the calcium-binding fluorophore Fluo-3 when preloaded cells were stimulated with CCL2. THP-1 cells were resuspended in serum-free RPMI 1640 medium at a density of 2×10^6 cells/mL. Cells were loaded with 3 μM of Fluo-3AM (Sigma-Aldrich) and 0.1% F127 and incubated at 37 °C for 30 min. The cells were washed twice to remove excess fluorophore, resuspended in serum-free RPMI 1640 medium at a density of 5×10^6 cells/mL, and kept at room temperature. Cells were pretreated with either DMSO or test compound for 30 min. To detect intracellular calcium fluxed by flow cytometry, pretreated cells were collected for 15 s and then continuously from 20 to 120 s after adding 100 ng/mL hCCL2, and the fluorescence shift was monitored. The inhibition achieved by increasing the concentration of test compound was calculated as a percentage of the compound-free DMSO control.

Thioglycolate-Induced Peritonitis in Mice. Six-week-old male ICR mice (n = 5) were injected intraperitoneally with 2 mL of 3% Brewer's thioglycollate broth (Difco, Detroit, MI). The test compounds were administered subcutaneously immediately after the thioglycollate injection and then again at 3 and 6 h. An anti-CCL2 antibody was used as a positive control. Three days after the thioglycollate administration, the mice were sacrificed and the total number of elicited cells and MOMA2 positive cells in the peritoneal exudates were analyzed using a Beckman Coulter Epics XL flow cytometer.

Delayed-Type Hypersensitivity (DTH) Response in Mice. Six-week-old male ICR mice ($n = 8$) were first immunized by intravenous administration of 1×10^6 sheep red blood cells (SRBC) and 4 days later challenged with 2×10^8 SRBC administered intradermally on their footpad. Vehicle or test compound was given orally 1 h prior to and 2 h after challenge, and the footpad thickness was measured on day 5 using a plethysmometer. Swelling was quantified as the mean percentage of footpad thickness relative to that of the vehicle-treated group.

Collagen-Induced Arthritis (CIA) in Rat. CIA was induced in 6-week-old female Lewis SPF rats ($n = 8$/group) by intradermal injection at the base of the tail of 900 μg of bovine tail tendon type II collagen (Collagen Gijutsu Kenshukai, Tokyo, Japan) emulsified in 600 μL of Freund's complete adjuvant (Difco, Detroit, U.S.) containing 4 mg/mL *Mycobacterium tuberculosis* on day 0 and boosted with another injection of 450 μg/300 μL of the collagen emulsion on day 7. Rats were dosed twice daily by gavage with the test compound suspended in 5% (w/v) aqueous gum arabic (GA) or an equal volume of GA solution; methotrexate, given 3 times per week, was used as a positive control. The volume of the rat's hind limbs was measured with a plethysmometer on days 0, 12, 14, 21, and 28, and inflammation was quantified as the mean percentage of increased volume over that at day 0. On day 29, the animals were sacrificed and radiographs of the hind paws were taken to assess the extent of bone destruction. Assessment was made in a blind manner using the following scale: 0, normal; 1, slight damage; 2, mild; 3, obvious damage; 4, marked bone destruction. The average of both legs was calculated and assigned as the score of the bone destruction.

Adjuvant-Induced Arthritis (AIA) in Rat. AIA was induced in 6-week-old female Lewis SPF rats ($n = 8$/group) by intradermal injection into the footpad of the right hind paw of 100 μL of PBS-emulsified Freund's complete adjuvant (Difco, Detroit, U.S.) containing 10 mg/mL *Mycobacterium butyricum*. Starting on day 10 after the immunization, rats were dosed twice daily by gavage with the test compound suspended in 5% (w/v) aqueous gum arabic (GA) or an equal volume of vehicle; methotrexate, given 3 times per week, was used as a positive control. The volume of the left hind limbs of the rats was measured with a plethysmometer on days 0, 8, 15, 21, and 28, and inflammation was quantified as the mean percentage of increased volume over that at day 0.

Experimental Autoimmune Encephalomyelitis (EAE) in Mice. EAE was induced in C57BL/6 mice ($n = 10$/group) by subcutaneous injection into the flanks of 150 μg of encephalitogenic peptide MOG_{35-55} (MEVGWYRSPFSRVVHLYRNGK; Auspep, Melbourne, Australia) emulsified in Freund's complete adjuvant (Difco, Detroit, U.S.) containing 4 mg/mL of *Mycobacterium tuberculosis*. Mice were then immediately injected intravenously with 350 ng of pertussis vaccine (List Biological Laboratories, Campbell, U.S.) and again 48 h later. Compounds were dissolved in 3% aqueous Tween 80 at 4 mg/mL and stored at 4 °C. Starting on the day of immunization (day 0), mice were dosed b.i.d. with test compound or an equal volume of water given orally and monitored daily for neurological impairment. Clinical scoring was based on an arbitrary scale of 0–5 as follows: 0, no detectable impairment; 1, flaccid tail; 2, hind limb weakness; 3, hind limb paralysis; 4, hind limb paralysis and ascending paralysis; 5, moribund or dead. A semiquantitative assessment of histological lesions was performed at the end of the study by staining sections of the brain and spinal cord with hematoxylin and eosin and scoring them using the following scale: 0, no inflammation; 1, few very small cellular infiltrate in the perivascular areas and meninges; 2, mild cellular infiltrate; 3, moderate cellular infiltrate; 4, severe cellular infiltrate; 5, very large and extensive cellular infiltrate.

Statistical Analysis. Statistical significance of differences between mean values of compound-treated and control groups was analyzed using the paired two-tailed *t* test with significance set at *p* values below 0.05 (∗, *p* < 0.05; ∗∗, *p* < 0.01).

■ ASSOCIATED CONTENT

ⓢ Supporting Information. Analytical data (HPLC, MS, and ^{1}H NMR) for compounds **8**, **10**, and **12**; AST and ALT values and histological changes in liver and kidney observed with **17** at 300 mg/kg. This material is available free of charge via the Internet at http://pubs.acs.org.

■ AUTHOR INFORMATION

Corresponding Author

*Phone: 650-845-7752. Fax: 650-845-7800. E-mail: elaborde@telik.com.

■ ACKNOWLEDGMENT

■ DEDICATION

[†]We dedicate this manuscript to the memory of Dr. Reinaldo ("Rey") Gomez.

■ ABBREVIATIONS USED

AIA, adjuvant-induced arthritis; CIA, collagen-induced arthritis; CCL2, C–C chemokine ligand 2; CCR2, C–C chemokine receptor 2; DTH, delayed-type hypersensitivity; EAE, experimental autoimmune encephalomyelitis; GPCR, G-protein-coupled receptor; IU/L, international units per liter; MCP-1, monocyte chemoattractant protein 1; MOG, myelin oligodendrocyte glycoprotein; MS, multiple sclerosis; RA, rheumatoid arthritis; SD, standard deviation; TRAP, target-related affinity profiling

■ REFERENCES

(1) Butcher, E. C. Leukocyte-endothelial cell recognition: three (or more) steps to specificity and diversity. *Cell* **1991**, *67* (6), 1033–1036.

(2) Foxman, E. F.; Campbell, J. J.; Butcher, E. C. Multistep navigation and the combinatorial control of leukocyte chemotaxis. *J. Cell Biol.* **1997**, *139* (5), 1349–1360.

(3) Butcher, E. C. The Multistep Model of Leukocyte Trafficking: A Personal Perspective from 15 Years Later. In *Leukocyte Trafficking. Molecular Mechanisms, Therapeutic Targets, and Methods*; Hamann, A., Engelhardt, B., Eds.; Wiley-VCH: Weinhem, Germany, 2005.

(4) Petri, B.; Phillipson, M.; Kubes, P. The physiology of leukocyte recruitment: an in vivo perspective. *J. Immunol.* **2008**, *180* (10), 6439–6446.

(5) Wong, C. H.; Heit, B.; Kubes, P. Molecular regulators of leucocyte chemotaxis during inflammation. *Cardiovasc. Res.* **2010**, *86* (2), 183–191.

(6) Taub, D. D. Chemokine–leukocyte interactions. The voodoo that they do so well. *Cytokine Growth Factor Rev.* **1996**, *7* (4), 355–376.

(7) Baggiolini, M. Chemokines and leukocyte traffic. *Nature* **1998**, *392* (6676), 565–568.

(8) Fernandez, E. J.; Lolis, E. Structure, function, and inhibition of chemokines. *Annu. Rev. Pharmacol. Toxicol.* **2002**, *42*, 469–499.

(9) Murdoch, C.; Finn, A. Chemokine receptors and their role in inflammation and infectious diseases. *Blood.* **2000**, *95* (10), 3032–3043.

(10) Le, Y.; Zhou, Y.; Iribarren, P.; Wang, J. Chemokines and chemokine receptors: their manifold roles in homeostasis and disease. *Cell. Mol. Immunol.* **2004**, *1* (2), 95–104.

(11) Valente, A. J.; Graves, D. T.; Vialle-Valentin, C. E.; Delgado, R.; Schwartz, C. J. Purification of a monocyte chemotactic factor secreted by nonhuman primate vascular cells in culture. *Biochemistry* **1988**, *27* (11), 4162–4168.

(12) Matsushima, K.; Larsen, C. G.; DuBois, G. C.; Oppenheim, J. J. Purification and characterization of a novel monocyte chemotactic and activating factor produced by a human myelomonocytic cell line. *J. Exp. Med.* **1989**, *169* (4), 1485–1490.

(13) Carr, M. W.; Roth, S. J.; Luther, E.; Rose, S. S.; Springer, T. A. Monocyte chemoattractant protein 1 acts as a T-lymphocyte chemoattractant. *Proc. Natl. Acad. Sci. U.S.A.* **1994**, *91* (9), 3652–3656.

(14) Mahad, D. J.; Ransohoff, R. M. The role of MCP-1 (CCL2) and CCR2 in multiple sclerosis and experimental autoimmune encephalomyelitis (EAE). *Semin. Immunol.* **2003**, *15* (1), 23–32.

(15) Sørensen, T. L.; Ransohoff, R. M.; Strieter, R. M.; Sellebjerg, F. Chemokine CCL2 and chemokine receptor CCR2 in early active multiple sclerosis. *Eur. J. Neurol.* **2004**, *11* (7), 445–449.

(16) Mahad, D.; Callahan, M. K.; Williams, K. A.; Ubogu, E. E.; Kivisäkk, P.; Tucky, B.; Kidd, G.; Kingsbury, G. A.; Chang, A.; Fox, R. J.; Mack, M.; Sniderman, M. B.; Ravid, R.; Staugaitis, S. M.; Stins, M. F.; Ransohoff, R. M. Modulating CCR2 and CCL2 at the blood−brain barrier: relevance for multiple sclerosis pathogenesis. *Brain* **2006**, *129* (Part 1), 212–223.

(17) Koch, A. E.; Kunkel, S. L.; Harlow, L. A.; Johnson, B.; Evanoff, H. L.; Haines, G. K.; Burdick, M. D.; Pope, R. M.; Strieter, R. M. Enhanced production of monocyte chemoattractant protein-1 in rheumatoid arthritis. *J. Clin. Invest.* **1992**, *90* (3), 772–779.

(18) Villiger, P. M.; Terkeltaub, R.; Lotz, M. Production of monocyte chemoattractant protein-1 by inflamed synovial tissue and cultured synoviocytes. *J. Immunol.* **1992**, *149* (2), 722–727.

(19) Harigai, M.; Hara, M.; Yoshimura, T.; Leonard, E. J.; Inoue, K.; Kashiwazaki, S. Monocyte chemoattractant protein-1 (MCP-1) in inflammatory joint diseases and its involvement in the cytokine network of rheumatoid synovium. *Clin. Immunol. Immunopathol.* **1993**, *69* (1), 83–91.

(20) Ylä-Herttuala, S.; Lipton, B. A.; Rosenfeld, M. E.; Särkioja, T.; Yoshimura, T.; Leonard, E. J.; Witztum, J. L.; Steinberg, D. Expression of monocyte chemoattractant protein 1 in macrophage-rich areas of human and rabbit atherosclerotic lesions. *Proc. Natl. Acad. Sci. U.S.A.* **1991**, *88* (12), 5252–5256.

(21) Nelken, N. A.; Coughlin, S. R.; Gordon, D.; Wilcox, J. N. Monocyte chemoattractant protein-1 in human atheromatous plaques. *J. Clin. Invest.* **1991**, *88* (4), 1121–1127.

(22) Gu, L.; Okada, Y.; Clinton, S. K.; Gerard, C.; Sukhova, G. K.; Libby, P.; Rollins, B. J. Absence of monocyte chemoattractant protein-1 reduces atherosclerosis in low density lipoprotein receptor-deficient mice. *Mol. Cell* **1998**, *2* (2), 275–281.

(23) Daly, C.; Rollins, B. J. Monocyte chemoattractant protein-1 (CCL2) in inflammatory disease and adaptive immunity: therapeutic opportunities and controversies. *Microcirculation* **2003**, *10* (3−4), 247–257.

(24) Kalinowska, A.; Losy, J. Investigational C-C chemokine receptor 2 antagonists for the treatment of autoimmune diseases. *Expert Opin. Invest. Drugs* **2008**, *17* (9), 1267–1279.

(25) Xia, M.; Sui, Z. Recent developments in CCR2 antagonists. *Expert Opin. Ther. Pat.* **2009**, *19* (3), 295–303.

(26) Pease, J. E.; Horuk, R. Chemokine receptor antagonists: part 1. *Expert Opin. Ther. Pat.* **2009**, *19* (1), 39–58.

(27) Beroza, P.; Damodaran, K.; Lum, R. T. Target-related affinity profiling: Telik's lead discovery technology. *Curr. Top. Med. Chem.* **2005**, *5* (4), 371–381.

(28) Tsuchiya, S.; Yamabe, M.; Yamaguchi, Y.; Kobayashi, Y.; Konno, T.; Tada, K. Establishment and characterization of a human acute monocytic leukemia cell line (THP-1). *Int. J. Cancer.* **1980**, *26* (2), 171–176.

(29) Kettle, J. G.; Faull, A. W.; Barker, A. J.; Davies, D. H.; Stone, M. A. *N*-Benzylindole-2-carboxylic acids: potent functional antagonists of the CCR2b chemokine receptor. *Bioorg. Med. Chem. Lett.* **2004**, *14* (2), 405–408.

(30) Pasternak, A.; Goble, S. D.; Struthers, M.; Vicario, P. P.; Ayala, J. M.; Di Salvo, J.; Kilburn, R.; Wisniewski, T.; DeMartino, J. A.; Mills, S. G.; Yang, L. Discovery of a potent and orally bioavailable CCR2 and CCR5 dual antagonist. *ACS Med. Chem. Lett.* **2010**, *1* (1), 14–18.

(31) Baba, M.; Nishimura, O.; Kanzaki, N.; Okamoto, M.; Sawada, H.; Iizawa, Y.; Shiraishi, M.; Aramaki, Y.; Okonogi, K.; Ogawa, Y.; Meguro, K.; Fujino, M. A small-molecule, nonpeptide CCR5 antagonist with highly potent and selective anti-HIV-1 activity. *Proc. Natl. Acad. Sci. U.S.A.* **1999**, *96* (10), 5698–5703.

(32) de Mendonça, F. L.; da Fonseca, P. C.; Phillips, R. M.; Saldanha, J. W.; Williams, T. J.; Pease, J. E. Site-directed mutagenesis of CC chemokine receptor 1 reveals the mechanism of action of UCB 35625, a small molecule chemokine receptor antagonist. *J. Biol. Chem.* **2005**, *280* (6), 4808–4816.

(33) Bertini, R.; Allegretti, M.; Bizzarri, C.; Moriconi, A.; Locati, M.; Zampella, G.; Cervellera, M. N.; Di Cioccio, V.; Cesta, M. C.; Galliera, E.; Martinez, F. O.; Di Bitondo, R.; Troiani, G.; Sabbatini, V.; D'Anniballe, G.; Anacardio, R.; Cutrin, J. C.; Cavalieri, B.; Mainiero, F.; Strippoli, R.; Villa, P.; Di Girolamo, M.; Martin, F.; Gentile, M.; Santoni, A.; Corda, D.; Poli, G.; Mantovani, A.; Ghezzi, P.; Colotta, F. Noncompetitive allosteric inhibitors of the inflammatory chemokine receptors CXCR1 and CXCR2: prevention of reperfusion injury. *Proc. Natl. Acad. Sci. U.S.A.* **2004**, *101* (32), 1791–1796.

(34) Ono, S. J.; Nakamura, T.; Miyazaki, D.; Ohbayashi, M.; Dawson, M.; Toda, M. Chemokines: roles in leukocyte development, trafficking, and effector function. *J. Allergy Clin. Immunol.* **2003**, *111* (6), 1185–1199.

(35) Hoover-Plow, J. L.; Gong, Y.; Shchurin, A.; Busuttil, S. J.; Schneeman, T. A.; Hart, E. Strain and model dependent differences in inflammatory cell recruitment in mice. *Inflammation Res.* **2008**, *57* (10), 457–463.

(36) Kuziel, W. A.; Morgan, S. J.; Dawson, T. C.; Griffin, S.; Smithies, O.; Ley, K.; Maeda, N. Severe reduction in leukocyte adhesion and monocyte extravasation in mice deficient in CC chemokine receptor 2. *Proc. Natl. Acad. Sci. U.S.A.* **1997**, *94* (22), 12053–12058.

(37) Boring, L.; Gosling, J.; Chensue, S. W.; Kunkel, S. L.; Farese, R. V., Jr.; Broxmeyer, H. E.; Charo, I. F. Impaired monocyte migration and reduced type 1 (Th1) cytokine responses in C-C chemokine receptor 2 knockout mice. *J. Clin. Invest.* **1997**, *100* (10), 2552–2561.

(38) Takahashi, M.; Galligan, C.; Tessarollo, L.; Yoshimura, T. Monocyte chemoattractant protein-1 (MCP-1), not MCP-3, is the primary chemokine required for monocyte recruitment in mouse peritonitis induced with thioglycollate or zymosan A. *J. Immunol.* **2009**, *183* (5), 3463–3471.

(39) Lu, B.; Rutledge, B. J.; Gu, L.; Fiorillo, J.; Lukacs, N. W.; Kunkel, S. L.; North, R.; Gerard, C.; Rollins, B. J. Abnormalities in monocyte recruitment and cytokine expression in monocyte chemoattractant protein 1-deficient mice. *J. Exp. Med.* **1998**, *187* (4), 601–608.

(40) Kraal, G.; Rep, M.; Janse, M. Macrophages in T and B cell compartments and other tissue macrophages recognized by monoclonal antibody MOMA-2. An immunohistochemical study. *Scand. J. Immunol.* **1987**, *26* (6), 653–661.

(41) Black, C. A. Delayed type hypersensitivity: current theories with an historic perspective. *Dermatol. Online J.* **1999**, *5* (1), 7.

(42) Williams, R. O. Collagen-induced arthritis as a model for rheumatoid arthritis. *Methods Mol. Med.* **2004**, *98*, 207–216.

(43) Ogata, H.; Takeya, M.; Yoshimura, T.; Takagi, K.; Takahashi, K. The role of monocyte chemoattractant protein-1 (MCP-1) in the pathogenesis of collagen-induced arthritis in rats. *J. Pathol.* **1997**, *182* (1), 106–114.

(44) Brühl, H.; Cihak, J.; Schneider, M. A.; Plachý, J.; Rupp, T.; Wenzel, I.; Shakarami, M.; Milz, S.; Ellwart, J. W.; Stangassinger, M.; Schlöndorff, D.; Mack, M. Dual role of CCR2 during initiation and progression of collagen-induced arthritis: evidence for regulatory activity of CCR2+ T cells. *J. Immunol.* **2004**, *172* (2), 890–898.

(45) van Eden, W.; Wagenaar-Hilbers, J. P. A.; Wauben, M. H. M. Adjuvant arthritis in the rat. *Curr. Protoc. Immunol.* **2001**, Unit 15.4, DOI: 10.1002/0471142735.im1504s19.

(46) Shahrara, S.; Amin, M. A.; Woods, J. M.; Haines, G. K.; Koch, A. E. Chemokine receptor expression and in vivo signaling pathways in the joints of rats with adjuvant-induced arthritis. *Arthritis Rheum.* **2003**, *48* (12), 3568–3583.

(47) Liu, S. H.; Wong, C. S.; Chang, D. M. Increased monocyte chemoattractant protein-1 in knee joints of rats with adjuvant-induced arthritis: in vivo microdialysis. *J. Rheumatol.* **2005**, *32* (11), 2205–2211.

(48) Shahrara, S.; Proudfoot, A. E.; Park, C. C.; Volin, M. V.; Haines, G. K.; Woods, J. M.; Aikens, C. H.; Handel, T. M.; Pope, R. M. Inhibition of monocyte chemoattractant protein-1 ameliorates rat adjuvant-induced arthritis. *J. Immunol.* **2008**, *180* (5), 3447–3456.

(49) Swanborg, R. H. Experimental autoimmune encephalomyelitis in rodents as a model for human demyelinating disease. *Clin. Immunol. Immunopathol.* **1995**, *77* (1), 4–13.

(50) Huang, D. R.; Wang, J.; Kivisakk, P.; Rollins, B. J.; Ransohoff, R. M. Absence of monocyte chemoattractant protein 1 in mice leads to decreased local macrophage recruitment and antigen-specific T helper cell type 1 immune response in experimental autoimmune encephalomyelitis. *J. Exp. Med.* **2001**, *193* (6), 713–726.

(51) Fife, B. T.; Huffnagle, G. B.; Kuziel, W. A.; Karpus, W. J. CC chemokine receptor 2 is critical for induction of experimental autoimmune encephalomyelitis. *J. Exp. Med.* **2000**, *192* (6), 899–905.

(52) Izikson, L.; Klein, R. S.; Charo, I. F.; Weiner, H. L.; Luster, A. D. Resistance to experimental autoimmune encephalomyelitis in mice lacking the CC chemokine receptor (CCR)2. *J. Exp. Med.* **2000**, *192* (7), 1075–1080.

(53) Gaupp, S.; Pitt, D.; Kuziel, W. A.; Cannella, B.; Raine, C. S. Experimental autoimmune encephalomyelitis (EAE) in CCR2($-$/$-$) mice: susceptibility in multiple strains. *Am. J. Pathol.* **2003**, *162* (1), 139–150.

(54) Kennedy, K. J.; Strieter, R. M.; Kunkel, S. L.; Lukacs, N. W.; Karpus, W. J. Acute and relapsing experimental autoimmune encephalomyelitis are regulated by differential expression of the CC chemokines macrophage inflammatory protein-1alpha and monocyte chemotactic protein-1. *J. Neuroimmunol.* **1998**, *92* (1–2), 98–108.

(55) Brodmerkel, C. M.; Huber, R.; Covington, M.; Diamond, S.; Hall, L.; Collins, R.; Leffet, L.; Gallagher, K.; Feldman, P.; Collier, P.; Stow, M.; Gu, X.; Baribaud, F.; Shin, N.; Thomas, B.; Burn, T.; Hollis, G.; Yeleswaram, S.; Solomon, K.; Friedman, S.; Wang, A.; Xue, C. B.; Newton, R. C.; Scherle, P.; Vaddi, K. Discovery and pharmacological characterization of a novel rodent-active CCR2 antagonist, INCB3344. *J. Immunol.* **2005**, *175* (8), 5370–5378.

(56) Bernard, C. C.; Johns, T. G.; Slavin, A.; Ichikawa, M.; Ewing, C.; Liu, J.; Bettadapura, J. Myelin oligodendrocyte glycoprotein: a novel candidate autoantigen in multiple sclerosis. *J. Mol. Med.* **1997**, *75* (2), 77–88.

(57) Karnezis, T.; Mandemakers, W.; McQualter, J. L.; Zheng, B.; Ho, P. P.; Jordan, K. A.; Murray, B. M.; Barres, B.; Tessier-Lavigne, M.; Bernard, C. C. The neurite outgrowth inhibitor Nogo A is involved in autoimmune-mediated demyelination. *Nat. Neurosci.* **2004**, *7* (7), 736–744.

(58) Gong, J. H.; Ratkay, L. G.; Waterfield, J. D.; Clark-Lewis, I. An antagonist of monocyte chemoattractant protein 1 (MCP-1) inhibits arthritis in the MRL-lpr mouse model. *J. Exp. Med.* **1997**, *186* (1), 131–137.

(59) Jarnagin, K.; Grunberger, D.; Mulkins, M.; Wong, B.; Hemmerich, S.; Paavola, C.; Bloom, A.; Bhakta, S.; Diehl, F.; Freedman, R.; McCarley, D.; Polsky, I.; Ping-Tsou, A.; Kosaka, A.; Handel, T. M. Identification of surface residues of the monocyte chemotactic protein 1 that affect signaling through the receptor CCR2. *Biochemistry* **1999**, *38* (49), 16167–16177.

(60) Gavrilin, M. A.; Gulina, I. V.; Kawano, T.; Dragan, S.; Chakravarti, L.; Kolattukudy, P. E. Site-directed mutagenesis of CCR2 identified amino acid residues in transmembrane helices 1, 2, and 7 important for MCP-1 binding and biological functions. *Biochem. Biophys. Res. Commun.* **2005**, *327* (2), 533–540.

(61) May, L. T.; Leach, K.; Sexton, P. M.; Christopoulos, A. Allosteric modulation of G protein-coupled receptors. *Annu. Rev. Pharmacol. Toxicol.* **2007**, *47*, 1–51.

(62) Kenakin, T.; Miller, L. J. Seven transmembrane receptors as shapeshifting proteins: the impact of allosteric modulation and functional selectivity on new drug discovery. *Pharmacol. Rev.* **2010**, *62* (2), 265–304.